ELSEVIER

Biochimica et Biophysica Acta 1327 (1997) 193–203

BIOCHIMICA ET BIOPHYSICA ACTA
BBA

Isolation and characterization of the mitochondrial channel, VDAC, from the insect *Heliothis virescens*

Jan Ryerse [a,*], Marco Colombini [b], Timothy Hagerty [a], Barbara Nagel [a], Tong Tong Liu [b]

[a] *Department of Pathology, St. Louis University Health Sciences Center, 1402 South Grand Boulevard, St. Louis, MO 63104, USA*
[b] *Department of Zoology, University of Maryland, College Park, MD 20742, USA*

Received 22 October 1996; revised 10 February 1997; accepted 27 February 1997

Abstract

A 31 kDa voltage-dependent anion-selective channel (VDAC) protein was purified from the insect *Heliothis virescens* (tobacco budworm, denoted TBW) using an alkali extraction and filtration procedure and was characterized by SDS-PAGE, amino acid sequencing, biophysical properties and immunocytochemistry. The N-terminal sequence has highest identity with VDACs from mammals (50–66%) followed by plants (34–41%) and lower eukaryotes (30–34%). Reconstitution in planar phospholipid membranes yielded properties typical of VDACs from other organisms including a single-channel conductance of 4.1 nS (in 1 M KCl), closure in response to positive and negative transmembrane voltage, and a reversal potential of 11.8 mV indicating anion selectivity in the open state. A polyclonal antiserum (R19) raised against gel-purified 31 kDa protein specifically labelled mitochondria and mitochondrial outer membranes in TBW flight muscle by light and electron microscope immunocytochemistry. © 1997 Elsevier Science B.V.

Keywords: Voltage-dependent anion-selective channel; Insect; SDS-PAGE; N-terminal sequence; Biophysics; Immunocytochemistry

1. Introduction

Voltage-dependent anion-selective channels (VDACs; mitochondrial porins) transport adenine nucleotides and other anions and metabolites across the outer mitochondrial membrane in eukaryotes [1–5]. The structural component of the VDAC is an ~31 kDa protein which is thought to form a thin-walled β-barrel and includes an N-terminal α-helix [1,6–8]. The biophysical properties of VDACs from a variety of species have been characterized in planar phospholipid membranes and are highly conserved. Notable features include a unit conductance of ~4.0 nS in 1.0 M KCl, an anion selectivity in the open state and a voltage dependence reflected by a transition to a closed state when 20–30 mV potentials are applied in either direction across the membrane [2,3,9]. The 'closed' states remain permeable to small anions but are impermeable to organic ions such as ATP (T. Rostovtseva and M. Colombini, unpublished data).

Abbreviations: BSA, bovine serum albumin; CAPS, 3-(cyclohexylamino)-1-propanesulfonic acid; DW, distilled water; EM, electron microscopy; HB, homogenization buffer; OG, octyl β-D-glucopyranoside; LM, light microscopy; Mes, 2-(*N*-morpholino)ethanesulfonic acid; SDS, sodium dodecylsulfate; TBW, tobacco budworm; NADH, nicotinamide adenine dinucleotide; PBS, phosphate-buffered saline; VDAC, voltage-dependent anion-selective channel

* Corresponding author. Fax: +1 (314) 5778489. E-mail: ryersejs@slu.edu

0005-2736/97/$17.00 © 1997 Elsevier Science B.V. All rights reserved.
PII S0005-2736(97)00058-8

Biophysical characterization of wild-type and mutant VDACs expressed in yeast have advanced our understanding of VDAC structure and function [3,8]. VDACs have been believed by some to be simple passive conduits, but mounting evidence suggests that VDACs may be regulated by voltage [10], cytoplasmic enzymes [11], a modulator protein [12,13], and by cellular metabolites such as NADH [14,15] and ATP [16]. Questions concerning mechanisms by which VDACs are regulated in multicellular eukaryotes in vivo have not been widely addressed because of the lack of convenient multi-cellular models in which the consequences of knocking out or otherwise manipulating VDACs can be evaluated. Arthropods would be attractive models for such studies [17], however, there have been few reports of VDACs in insects or other arthropods [18,19].

The objectives of this study were to purify and characterize a VDAC protein from an insect and to develop probes which could be used to clone arthropod VDAC genes for molecular characterization. We chose the tobacco budworm, *Heliothis virescens* (denoted TBW) because it is a relatively large insect and thus provides abundant protein for analysis and for raising antibodies, and because it can be conveniently reared in quantity. In this report, we describe a method to purify TBW VDAC protein which does not require mitochondrial isolation or column chromatography as is typically used by others [7] and we describe a polyclonal antibody raised against the TBW VDAC protein. The protein is assigned VDAC status based on molecular mass, partial amino acid sequence, biophysical properties and immunocytochemistry. The antibody was used in an expression screen to identify a VDAC cDNA from *Drosophila melanogaster* which is described in the companion paper [20].

2. Materials and methods

2.1. Experimental animals

Tobacco budworm larvae (*Heliothis virescens*; Lepidoptera: Nymphalidae; denoted TBW), reared on artificial diet, were obtained from the insectary at Monsanto Company, St. Louis, MO. Fifth stage larvae were collected and stored at -20°C.

2.2. Purification of VDAC protein

The isolation procedure was modified from that used to purify gap junctions [21]. Four g batches of frozen TBW larvae were cut into pieces with a razor and homogenized in 10 ml of homogenization buffer (denoted HB; 1 mM sodium bicarbonate, pH 7.2 with 5 μg/ml phenylthiourea to inhibit phenolase activity and 1 μg/ml aprotinin, 0.25 mg/ml ethylenediaminetetraacetic acid, 1 μg/ml leupeptin, 0.7 μg/ml pepstatin A, 5 μg/ml phenylmethylsulfonyl fluoride and 5 μg/ml soybean trypsin inhibitor as proteinase inhibitors) with 7 strokes in a 40 ml Pyrex glass homogenizer. Homogenates were strained through a metal sieve to remove large pieces of cuticle and other debris and the filtrate was centrifuged at $500 \times g$ in a clinical centrifuge for 3 min. The supernatant was pelleted in a Beckman Ti-50 rotor at $10\,000 \times g$ and washed twice in HB. The pellet was resuspended in 2.75 ml of HB and mixed well with 4.25 ml of 60% sucrose. The solution was added to a 10 ml Beckman Ti-50 centrifuge tube, overlaid with 2 ml of 30% sucrose and 2 ml of HB, and centrifuged for 45 min at $100\,000 \times g$. Crude membranes at the 30/42% interface were collected and washed in HB. All of the preceding steps were at 4°C and all subsequent steps were at room temperature unless noted otherwise. The pellets were resuspended in 1 ml of 2.5 mM NaOH in DW in a microcentrifuge tube, mixed for 1–2 min by pipetting and centrifuged in a microfuge at full speed for 5 min. The pellets were washed once in HB. In some cases the NaOH pellets were resuspended in HB and filtered through 60 and 8 μm filters [22] to remove small fragments of cuticle and basal lamina, and in some cases the NaOH or NaOH/filtered pellets were solubilized in n-octyl β-D-glucopyranoside (denoted OG, US Biochemical) to extract membrane proteins. For this purpose, the pellets were resuspended in 1 ml of 1% OG in HB, vortexed, incubated for 3 min and centrifuged for 5 min. The supernatant was transferred to a fresh microcentrifuge tube and 250 μl of 40% trichloroacetic acid was added to precipitate soluble protein. The solution was vortexed, incubated for 10 min at 4°C and centrifuged for 5 min. The pellet was washed twice in distilled water.

Total protein yields (mean $\pm$ 1 standard deviation, $n = 3$) per g of larvae were 3.2 ± 0.1 mg for crude

membrane, 49.2 ± 4.2 μg for the NaOH pellet and 13.0 ± 1.5 μg for the NaOH/OG/TCA pellet. Protein assays were carried out using the Pierce Micro BCA kit with samples solubilized in 2% SDS and with bovine serum albumin in 2% SDS as protein standard.

2.3. Electrophoresis, electrotransfer and electro-elution

For SDS-PAGE, pellets containing ~ 100 μg of protein were solubilized in 80 μl of SDS electrophoresis sample buffer [23], boiled and centrifuged for 3 min each and electrophoresed in 6% stacking over 12% resolving polyacrylamide gels in a Bio-Rad mini-electrophoresis apparatus at 150 volt (V). For immunoblots, unstained gels were equilibrated 2×5 min in CAPS buffer [24], pH 11 and electrotransferred to 0.45 μm nitrocellulose membranes in CAPS buffer in a Bio-Rad mini-transfer apparatus at 0.35 amp for 60 min. The membrane was rinsed in DW, air-dried and stored at -20°C until staining. For electro-elution, the 31 kDa protein band was excised from Coomassie blue-stained gels and placed in 2 ml of elution buffer (0.025 M Tris, 0.2 M glycine, pH 8.2 containing 0.1% SDS) in 12 kDa dialysis tubing. The dialysis bag was submerged in elution buffer in an agarose gel apparatus and the protein eluted at 40 V for 1 h. The eluate was dialyzed 2×12 h against DW and concentrated 10-fold in a SpeedVac. An aliquot was evaluated by SDS-PAGE for purity and concentration, and the remainder was stored at -20°C.

2.4. N-terminal amino acid sequencing

For N-terminal amino acid sequencing unstained SDS-PAGE gels were transferred to Westran polyvinylidene fluoride membrane (Schleicher and Schuell) as described above for nitrocellulose. The membrane was rinsed in DW, stained with 1% Ponceau S in 1% acetic acid, destained in 1% acetic acid and washed in DW. The 31 kDa band was excised and sequenced in an Applied Biosystems 477A sequencer.

2.5. Biophysical characterization

Channels were reconstituted into planar phospholipid membranes by spontaneous insertion from the aqueous medium. The membranes were made by the monolayer method [25] as previously described [26] using lipids consisting of 5 parts asolectin to 1 part cholesterol. Five to 10 μl of NaOH-extracted sample were solubilized in Triton X-100 and added to 4 to 5 ml of 1 M KCl, 5 mM $CaCl_2$, 5 mM Mes pH 5.8, on one side of the membrane (cis side). The opposite (trans) side contained either 1 M KCl for single-channel measurements and voltage gating experiments or 0.1 M KCl for the selectivity experiments. The voltage was clamped [26] and the current recorded. The trans side was held at virtual ground so the voltage refers to the cis compartment. This is also the compartment to which VDAC samples were added. Calomel electrodes were used to interface with the solutions. The conductivity–voltage plot was generated by applying a triangular voltage wave at 5 mHz and using the current values recorded as the channels re-opened. The fast rates of opening allows for near equilibrium between the open state and the most readily accessible closed state.

2.6. Antiserum

A polyclonal antiserum (denoted R19) was raised in a rabbit. A 1:1 mix of TBW 31 kDa protein (eluted from SDS-PAGE gel strips as described above) and complete Freund's adjuvant was injected subcutaneously at multiple sites. Three weeks later the rabbit was boosted with a 1:1 mix of antigen and incomplete Freund's adjuvant. The rabbit was bled one week later and at bi-weekly intervals thereafter for a total of four bleeds. All bleeds exhibited a high titer antibody and a mixture of the four bleeds was used for experiments. Pre-immune and R19 sera were stored at -20°C. For affinity purification, ~ 100 μg of electro-eluted 31 kDa protein were coupled to Affigel beads (Bio-Rad) following the manufacturer's directions. Several milliliters of R19 antiserum were applied to the affinity column and after washing with PBS (0.15 M NaCl, 0.006 M Na_2HPO_4 and 0.004 M KH_2PO_4; pH 7.0) the bound antibody was eluted with 0.2 M glycine, pH 2.5, neutralized with NaOH

and stored at −20°C. The affinity purified antiserum is denoted R19AP.

2.7. R19 / R19AP immunoblots

Nitrocellulose membrane strips were rinsed in Tris-buffered saline (TBS, consisting of 0.02 M Tris (tris(hydroxymethyl)aminomethane) and 0.5 M NaCl, pH 8.5), blocked for 15 min in TBS containing 3% gelatin, washed 2 × 5 min in TBS containing 0.05% Tween-20 (TTBS), incubated for 60 min with anti-serum or pre-immune serum at various dilutions (see Section 3) in antibody buffer (TBS containing 1% gelatin), washed 3 × 5 min in TTBS, incubated for 30 min in alkaline phosphatase-conjugated goat anti-rabbit IgG diluted 1:1000 in antibody buffer, washed once in TBS and once in 0.1 M Tris (pH 9.5). Immunoreactive protein was visualized by incubating the strips for 5–20 min in freshly prepared enzyme reaction solution (0.25 mM *p*-nitro-blue tetrazolium chloride, 0.25 mM 5-bromo-4-chloro-3-indolyl phosphate toluidine salt, 0.5 mM $MgCl_2 \cdot 6H_2O$, pH 9.5). Stained strips were rinsed in DW and air dried.

2.8. R19 / R19AP immunocytochemistry

Adult TBW were anesthetized at 4°C and flight muscles dissected in cold PBS. The tissue was fixed in PBS containing 3.5% paraformaldehyde for 24 h and processed into plastic as described below or stored in fixative at 4°C.

For LM immunocytochemistry, the tissue was dehydrated through graded ethanols, embedded in LR White resin and polymerized with ultraviolet light for 16 h at −20°C. Thick (0.5 μm) sections were heat attached to glass slides, incubated for 15 min in a blocking solution of wash buffer (PBS containing 0.05% Tween-20) containing 3% ovalbumin, incubated with R19 or R19AP anti-serum or pre-immune serum diluted 1:500 or 1:100 in antibody buffer (wash buffer containing 1% ovalbumin) for 16 h at 4°C, washed 4 × 15 min in wash buffer, incubated in rhodamine-conjugated goat anti-rabbit IgG diluted 1:250 in antibody buffer for 1 h at RT and washed 4 × 15 min in PBS. Stained sections were mounted in FluoroSave-G (Southern Biotechnology Associates, Inc.), viewed with a Zeiss research light microscope equipped with fluorescence optics and photographed with Kodak T-MAX 400 ASA film.

For EM immunogold labelling of plastic-embedded tissue, silver to gold sections of LR White-embedded flight muscle were collected on parlodion-coated gold grids and the grids were floated section side down in drops of staining solution on parafilm in a covered petri dish at room temperature (unless noted otherwise) as follows: blocked in 3% BSA in PBS for 60 min, washed 5 × 1 min in PBS, incubated for 16 h at 4°C with R19AP or normal rabbit IgG at 5 μg/ml in PBS, washed 5 × 1 min in PBS, incubated in goat anti-rabbit IgG coupled to 10 nm colloidal gold (Bio-Cell Research) diluted 1:50 for 30 min, washed 5 × 1 min and air-dried. After post-staining with uranyl acetate and lead citrate the sections were viewed and photographed with a JEOL 100CX electron microscope at operated at 60 kV.

For EM immunogold labelling of frozen sections the tissue was fixed in 3.5% paraformaldehyde as described above, infiltrated with 3.2 M sucrose and frozen in liquid nitrogen. Thin sections were cut with a Reichert FC4D cryo-sectioning apparatus on a Reichert Ultracut E ultramicrotome and collected on formvar-coated nickel grids [27,28]. Sections were immunostained in 50 μl drops of solutions as follows: 1 × 1 min DW and PBS washes, blocked 3 × 10 min in 3% BSA in PBS, washed 1 × 1 min in 1% BSA in PBS, stained for 30 min with R19AP diluted 1:25 in 1% BSA in PBS, washed 4 × 1 min in 1% BSA in PBS, incubated for 30 min in goat anti-rabbit IgG–10 nM colloidal gold diluted 1:50 in 1% BSA in PBS, washed 4 × 1 min in PBS and 4 × 1 min in DW. Sections were stabilized and stained with methylcellulose containing 0.25% uranyl acetate and were viewed and photographed as described above.

3. Results

3.1. Purification of TBW VDAC protein

The purification procedure is based on the resistance of membranes containing a high density of transmembrane proteins to solubilization in dilute alkali [29]. VDACs are abundant in the outer mitochondrial membrane, with a density of 10^3–10^4 per square micron [30]. The procedure is modified from one used previously for gap junction-enriched fractions [21] and involves preparing a crude membrane fraction from larval homogenates by sucrose density

centrifugation, extracting the crude membranes with 2.5 mM NaOH, filtering through membrane discs containing progressively smaller pores and solubilizing the filtered pellet with octyl β-D-glucopyranoside (octyl glucoside, denoted OG). A single NaOH extraction does not significantly reduce the protein heterogeneity in the crude membrane fraction (Fig. 1, lane 2 vs. lane 1) but two NaOH extractions yield a fraction relatively enriched in the 31 kDa protein (Fig. 1, lane 3). Solubilization with 1% OG, (which solubilizes membrane proteins, Ref. [31]) after one NaOH extraction yields a fraction which is heterogeneous in protein content but contains an abundant 31 kDa protein (Fig. 1, lane 4). Solubilization with OG after two NaOH extractions yields essentially pure 31 kDa protein as judged by Coomassie blue staining (Fig. 1, lane 5). The preparations illustrated in Fig. 1, lanes 3 and 5 were filtered through 60 and 8 μm filters after NaOH extraction [22] which removes small fragments of cuticle and basal lamina and is required to obtain highly purified 31 kDa protein.

Chromatography of detergent extracts of isolated mitochondria over dry hydroxyapatite:celite columns [7] as used by others to purify VDAC protein was ineffective in purifying the TBW 31 kDa protein from NaOH, NaOH/OG or Triton X-100 fractions (not shown).

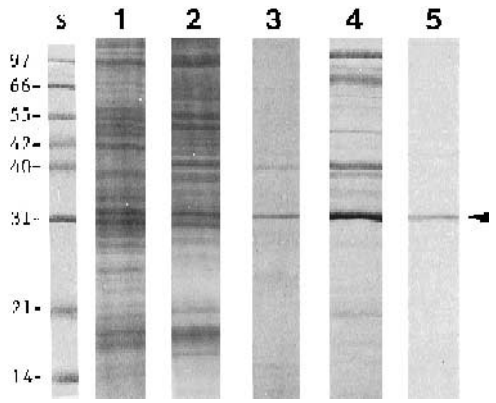

Fig. 1. Coomassie blue-stained SDS-PAGE gels of: lane 1, washed crude membranes; lane 2, crude membranes extracted 1× with 2.5 mM NaOH; lane 3, crude membranes extracted 2× with NaOH and filtered though 60 and 8 μm filters; lane 4, crude membranes extracted 1× with NaOH and then solubilized in octyl glucoside; lane 5, crude membranes extracted 2× with NaOH, filtered through 60 and 8 μm membrane filters and the filtrate pellet solubilized in octyl glucoside. Arrowhead, 31 kDa protein. Lane s, molecular mass standards in kDa.

	1 5 10 15 20 25 30	%ID	Ref
TBW	MA..PPYYADLGKKANDVESKG.YCFDVEKFDLK	-	-
Hpit	MAV.PPTYADLGKSARDVFTKG.YGFGLIKLDLK	66	[10]
Hlym	MAV.PPTYADLGKSARDVFTKG.YGFGLIKLDLK	66	[39]
Hmus	MAV.PPTYADLGKSARDVFTKG.YGFGLIKLDLK	66	[39]
D.m.	MA..PPSYSDLGKQARDIFSKG.YNFGLWKLDLK	65	[20]
Hliv§	MCI.PPSYADLGKVARDIFNKGF.GFGLVKLDVK	50	[10]
Rbr§	ICI.PPPYADLGKAARDIFNKGF.GFGLVKLDVK	50	[40]
Pea	MVKGPGLYTDIGKKARDLLYKD.YHSDK.KFTIS	41	[42]
Pot34	MGKGPGLYTEIGKKARDLLYKD.YQSDH.KFSTI	38	[41]
Maize	MVVAVGLYTDIGKKTRDLLYKD.YNTHQ.KFCLT	34	[42]
D.d.	MN..PGLYADLTKPTADFIKKDF.AETF.KLDTT	34	[43]
N.c.	MAV.PAFS.DIAKSANDLLNKDFYHLAAGTIEVK	31	[44]
S.c.	MSP.PV.YSDISRNINDLLNKDFYHATPAAFDVQ	30	[45]

Fig. 2. N-terminal sequence comparison of the TBW 31 kDa protein with VDACs from other species. %ID, % identity with the TBW sequence after alignment for maximum homology. Ref, reference. The N-terminal M was not present in the TBW sequence but is included for comparative purposes. Hpit, human pituitary (HVDAC1) [10]; Hlym, human lymphocyte (porin 31HL) [39]; Hmus, human skeletal muscle (porin 31HM) [39]; D.m., *D. melanogaster* [20]; Hliv, human liver (HVDAC2) [10]; Rbr, rat brain [40]; Pot34, potato 34 kDa protein (POM34) [41]; D.d., *D. discoideum* [43]; N.c., *N. crassa* [44]; S.c., *S. cerevisiae* [45]; pea and maize [42]. §, Hliv and Rbr contain 11 and 12 additional amino acids at the N-terminus which are not shown.

3.2. N-terminal amino acid sequence

The N-terminal amino acid sequence of the TBW 31 kDa protein is homologous with VDAC proteins from other species (Fig. 2). The TBW sequence has 65% identity with a predicted VDAC sequence from *D. melanogaster*, 50–66% identity with VDACs from mammals, 34–41% identity with VDACs from plants and 30–34% identity with VDACs from lower eukaryotes from the animal kingdom. Of the 13 conserved residues in the corresponding N-terminal domain of a VDAC consensus sequence [32], ten are conserved in the N-terminal sequence of the TBW protein.

3.3. Biophysical properties in planar phospholipid membranes

Protein fractions similar to those shown in Fig. 1, lanes 3 and 5 were introduced into planar phospholipid membranes in vitro. NaOH/filtered preparations yielded electro-physiological properties typical of VDAC proteins from other eukaryotes. The addition of 5 to 10 μl aliquots of this preparation (solubilized in 1% Triton X-100) to the aqueous solution (while stirring) on one side of a planar

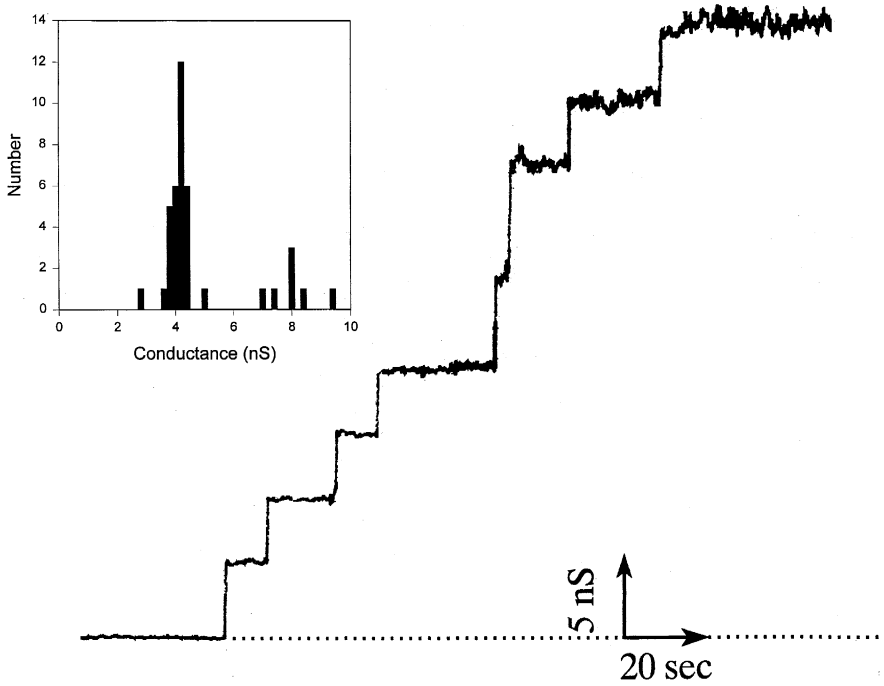

Fig. 3. Step increases in electrical conductance as single channels insert into the planar phospholipid membrane in vitro after addition of a 2× NaOH extracted/filtered TBW fraction solubilized in 1% Triton X-100. (Inset) The frequency–conductance histogram shows that the average magnitude of single-channel conductance is 4.1 nS. In a few cases two channels insert accounting for the higher conductance states.

phospholipid membrane resulted in the reconstitution of up to 30 channels into the membrane. The insertions produced the normal 'staircase' pattern due to high levels of preference for the high-conductance open state at low transmembrane voltages. The single-channel conductance was 4.1 nS (Fig. 3). As is frequently seen with VDAC from *Neurospora crassa* [33,34], the insertion of doublets was observed from time to time. This is responsible for the higher conductance events illustrated in the inset in Fig. 3. If smaller aliquots were added to the aqueous phase, single channels could be observed over prolonged periods. As is typical for VDACs, each channel exhibits two gating processes and thus each is capable of closure at both positive and negative voltages. This is best illustrated in recordings from membranes containing a single channel (Fig. 4). Changing the transmembrane potential from −10 to −50 mV results in an instantaneous current change due to the change in driving force. This is followed by a structural change that results in channel closure. The current drops not to zero but to a low value as the closed state is still conductive to small ions. This

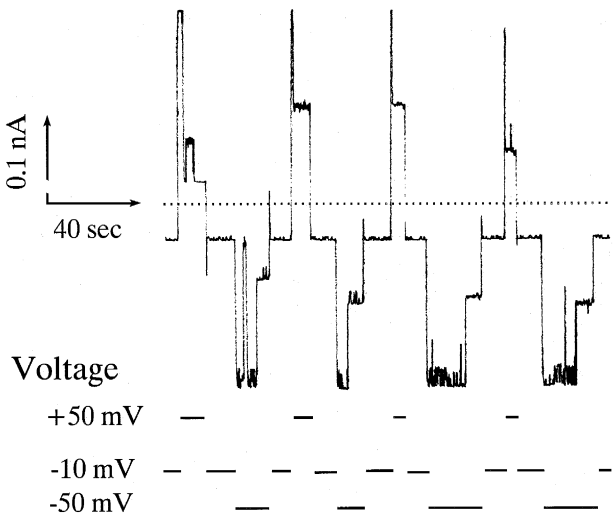

Fig. 4. Dependence of channel conductance on voltage. As transmembrane potential is altered from a potential of −10 mV to +50 mV or −50 mV the channels close. Conductance immediately returns to the open state with a return to −10 mV potential difference. The response time was limited by the recorder at 0.3 s for full scale response.

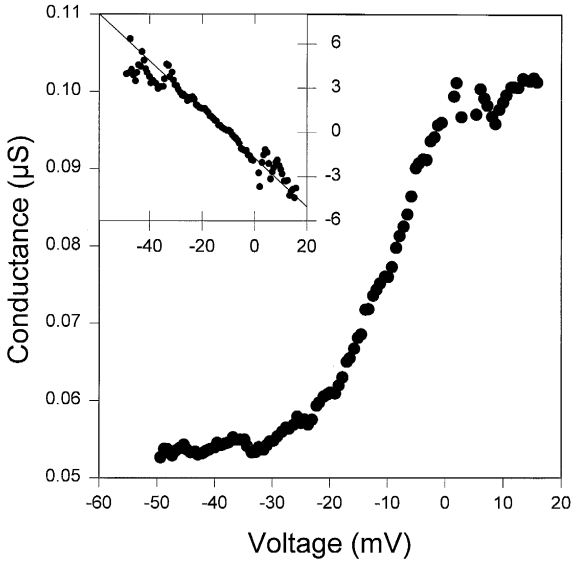

Fig. 5. Voltage–conductance curve showing increasingly greater negative potentials lead to channel closure. The inset shows the data fitted to a two-state model, a Boltzman distribution between the open and closed states as a function of voltage. The ordinate scale is $\ln(G_{max} - G / G - G_{min})$, where G_{max} = maximum conductance (all channels open), G_{min} = minimum conductance (all channels closed), G = conductance at any voltage. A linear fit indicates that the behavior of the channels is consistent with a two-state process. The voltage-dependent parameters of these data are: 'n' = 4.1, V_0 = 10.6 mV.

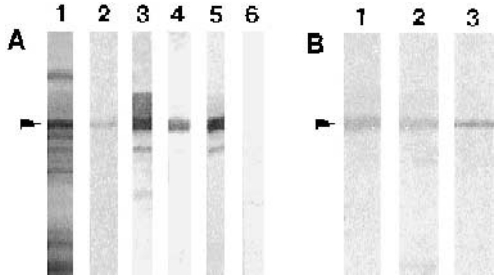

Fig. 6. (A) Lane 1, typical SDS-PAGE gel (Coomassie blue-stained) from which strips of 31 kDa protein were excised for elution and from which blots were prepared; lane 2, Coomassie blue-stained SDS-PAGE gel of electro-eluted 31 kDa protein used as antigen; lanes 3–6 immunoblots stained with R19 at 1:33 000 (lane 3), R19 at 1:500 000 (lane 4), R19AP at 1:5000 (lane 5) and pre-immune serum at 1:33 000 (lane 6). (B) Immunoblots stained with R19AP at 1:5000. Lane 1, crude membranes; lane 2, 1× NaOH extracted crude membranes; lane 3, crude membranes extracted 1× with NaOH and solubilized in 1% octyl glucoside. Arrow, position of the 31 kDa band. Alkaline phosphatase-conjugated secondary antibody and colorimetric enzyme reaction used to visualize immunoreactive bands.

closed-state conductance is variable as is the case for VDAC from other sources [9]. The rate of closure is evidently slow despite the stochastic nature of single channels. This reflects the slow decay in conductance seen in multi-channel membranes (not shown) and again, is typical of VDACs as is the rapid re-opening when the magnitude of the voltage is reduced. Note that in Fig. 4 the current returns immediately to the value recorded at −10 mV prior to raising the voltage. As is traditional for VDAC analysis, by taking advantage of the fast rates of opening, the steady-state dependence of conductance on voltage was obtained for one gating process (Fig. 5). Although closure occurs at positive potentials, the slower kinetics and electrical instability at high potentials made the recording of a reliable conductance/voltage plot difficult. The inset in Fig. 5 shows the data fitted to a 2-state process which allowed estimation of the voltage-dependence parameters: the steepness of the voltage gradient, n, and the mid-point of the voltage-switching region, V_0. The mean values were 3.3 and 15 mV, respectively, and well within the normal range of values reported for VDACs [3,9,35]. Traditionally, selectivity is estimated by measuring the voltage needed to bring the current to zero in the

Table 1
Comparison of biophysical properties of the TBW 31 kDa protein in planar phospholipid membranes with human and yeast VDACs

Species	TBW	Human	Yeast
Single-channel conductance in 1 M KCl (nS)	4.1 ± 0.3 (32)	4.1 ± 0.1 (16)	4.2 ± 0.1 (3)
Reversal potential (mV)	11.8 ± 0.3 (5)	11.1 ± 0.6 (5)	11.0 ± 0.2 (6)
Voltage sensitivity	+3.4	2.2 ± 0.4 (4)	2.5 ± 0.3 (7)
'n' value	−3.3 ± 0.5 (4)	2.4 ± 0.3 (3)	2.4 ± 0.5 (7)

The reversal potential is the potential required to bring the current to zero with 1 M and 0.1 M KCl in the cis and trans bath compartments and indicates anion selectivity. The 'n' value is the voltage sensitivity as determined by the steepness of the voltage-dependent conductance states for positive and negative transmembrane voltages. Data reported as mean ± 1 S.D. (n). Human = HVDAC1. Human and yeast data from Ref. [10].

presence of a 10-fold KCl gradient (1.0 M vs. 0.10 M KCl). While this underestimates the selectivity under physiological conditions, this value can be easily compared to literature values [3,9,35] for VDAC from very diverse species. An average of 11.8 mV is almost identical to the literature values and indicates anion selectivity. As summarized in Table 1, the biophysical data for the 31 kDa protein is similar to the properties of human and yeast VDACs and supports the conclusion that the TBW protein is VDAC. OG-solubilized fractions did not form channels in phospholipid membranes which may be attributed to conformational alterations which prevented membrane insertion or interfered with charge carrying ability.

3.4. R19 / R19AP immunoblots

A polyclonal antiserum, denoted R19, was raised against 31 kDa protein eluted from excised gel strips (Fig. 6A, lanes 1, 2). R19 exhibited intense staining of the 31 kDa protein on immunoblots at 1:33 000 (Fig. 6A, lane 3) and also exhibited significant staining at dilutions as great as 1:500 000 (Fig. 6A, lane 4). In addition, R19 stained an ~28 kDa protein which is likely a breakdown fragment of the 31 kDa protein. Control, pre-immune serum diluted 1:33 000 was negative on immunoblots (Fig. 6A, lane 6). Immunoblots stained with the affinity purified antiserum R19AP at 1:5000 had less background staining compared with the crude R19 antiserum (Fig. 6A,

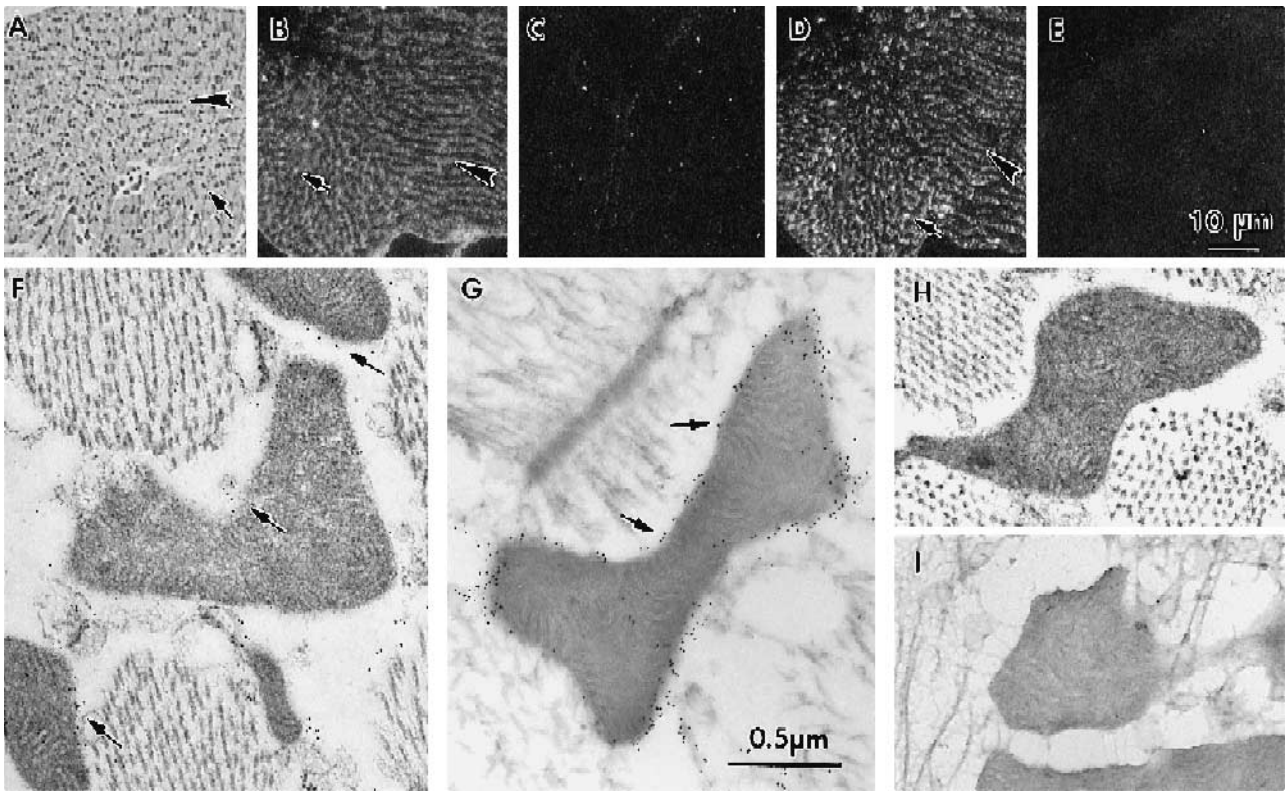

Fig. 7. Light (A–E) and electron (F–I) micrographs of R19 and R19AP immunostained TBW flight muscle. (A) Light micrograph of a 0.5 μm LR White section showing longitudinally-sectioned (arrowhead) and cross-sectioned (arrow) mitochondria. Toluidine blue-stained. (B) and (D) show immunofluorescent images of adjacent sections stained with R19 and R19AP, respectively, followed by a rhodamine-conjugated secondary antibody. Note columns (arrowheads) and profiles (arrows) of stained mitochondria. (C) and (E) show pre-immune serum and normal rabbit IgG controls which are negative for mitochondrial staining. (F) and (H) show mitochondria in thin plastic sections of muscle reacted with R19AP and normal rabbit IgG, respectively, followed by colloidal gold-labelled secondary antibody. Note the association of gold label primarily with the mitochondrial periphery in (F) (arrows) and no staining in (H). (G) and (I) show thin cryo-sections of mitochondria in muscle stained with R19AP or normal rabbit IgG. In (G), note abundance of gold label along the mitochondrial periphery and specific staining of the outer mitochondrial membrane in suitably cross-sectioned areas (arrows). Control IgG shown in (I) is negative. (A–E), 10 μm bar; (F–I), 0.5 μm bar.

lane 5). Fig. 6B illustrates R19-staining of the VDAC protein on immunoblots of crude membrane (lane 1), unfiltered NaOH (lane 2) and unfiltered NaOH/OG (lane 3) fractions.

3.5. R19 / R19AP immunocytochemistry

As further confirmation that the 31 kDa protein is a VDAC protein, sections of TBW flight muscle were stained with R19 and R19AP. Flight muscle was chosen because of the abundance and simple arrangement of the mitochondria in this tissue. In longitudinal sections, the mitochondria are arranged in rows between myocytes (Fig. 7A, arrowhead) whereas in transverse sections they appear as circular or elongate profiles encircling muscle cells (Fig. 7A, arrow). For immunofluorescence, 0.5 μm-thick sections of LR White-embedded flight muscle were stained with R19 or R19AP and rhodamine-conjugated secondary antibody. The staining pattern is consistent with the shape and distribution of mitochondria in the tissue (Fig. 7B,D). In some instances a 'rim' of staining is apparent around the mitochondrial periphery. The affinity purified serum yielded a crisper image with less background staining compared with the crude antiserum (Fig. 7D vs. Fig. 7B). Pre-immune serum and normal rabbit IgG controls were negative for mitochondrial staining (Fig. 7 C and E, respectively).

At the EM level, mitochondrial staining was observed in thin sections of LR White-embedded tissue and thin cryo-sections after incubation with R19AP and 10 nm colloidal gold-labelled secondary antibody. Labelling of the mitochondrial periphery is apparent in sections of LR White-embedded flight muscle (arrows in Fig. 7F), however membranes are poorly preserved due to lack of osmium fixation and membrane extraction during subsequent tissue processing. In cryo-sections of paraformaldehyde fixed tissue, on the other hand, the peripheral membranes of the mitochondria are well-preserved and label heavily with colloidal gold (Fig. 7G). In areas where the membranes are precisely cross-sectioned (e.g., arrows in Fig. 7G) specific labelling of the outer mitochondrial membrane is apparent. No mitochondrial staining was observed above background with normal rabbit IgG at the same concentration as R19AP (Fig. 7 H and I, respectively). Staining with crude anti-serum and pre-immune serum gave the same (positive and negative) mitochondrial staining as for R19AP and normal rabbit IgG except that non-specific background was higher (not shown).

4. Discussion

VDAC proteins have been characterized from a variety of plants and animals and comprise a family of related proteins. VDACs isolated from various species have molecular masses of 29 to 36 kDa by SDS-PAGE but typically are 29 to 31 kDa in size based on sequencing studies. We have isolated and characterized a VDAC protein from the tobacco budworm *H. virescens* (TBW) with an apparent molecular mass of 31 kDa by SDS-PAGE. This is the second characterization of a VDAC protein from an arthropod, a 31 kDa VDAC having been isolated from *D. melanogaster* [18]. In addition, the present report is the first to describe VDAC immunolocalization in any insect or arthropod.

Comparison of the N-terminal 31 amino acids of the TBW VDAC protein with VDACs from other species indicates that the TBW sequence has highest identity with VDACs from *D. melanogaster* and mammals followed by VDACs from plants and lower eukaryotes (Fig. 2). The 35% difference in sequence between TBW and the fly may be due to sequencing errors, it being unlikely that the TBW and fly sequences would have diverged to a greater extent than the 25% difference between flies and mammals. The N-terminal methionine residue is included in Fig. 2 for comparative purposes, however it was not detected in the sequence indicating cleavage during protein maturation. The relatively high degree of N-terminal homology with mammalian VDACs may reflect the presence of similar domains for targeting or regulation. A consensus sequence has been defined for the VDAC protein [32], and 10 of the 13 conserved residues in the N-terminal domain of the consensus sequence are conserved in the TBW protein. The absolute conservation of the aspartic acid and lysine residues at positions 17 and 21 among animals and plants suggest these play an essential role in channel function, probably in ion selectivity [8] since both are charged. The N-terminal homology with VDACs from other species provided encourag-

ing evidence that the TBW 31 kDa protein was a VDAC family member and prompted efforts to purify the protein for characterization in planar phospholipid membranes and for use as antigen.

A widely-used method for the purification of VDAC protein is hydroxyapatite:celite chromatography of mitochondrial detergent extracts [7]. However, application of this procedure to *D. melanogaster* larvae (Fig. 1A in [18]) generated a highly heterogeneous protein fraction rather than pure protein and we pursued an alternative approach. In previous studies, we extracted insect membrane preparations with alkali to obtain gap junction fractions. A 31 kDa protein was observed on SDS-PAGE gels of the fractions and was identified by amino acid sequencing as a candidate VDAC protein [36]. The procedure was modified to obtain enriched or purified 31 kDa VDAC fractions by incorporating sequential NaOH extractions, filtration and OG extraction. Purity and yield depend on the number and combination of NaOH extractions and filtrations employed. It was necessary to start with at least 25–50 g of larvae to obtain μg amounts of the 31 kDa protein.

Incorporation of NaOH/filtered fractions (e.g. Fig. 1, lane 3) into planar phospholipid membranes provided strong biophysical evidence that the 31 kDa protein is a VDAC protein. Values for the single-channel conductance, reversal potential and voltage dependence are similar to those from a variety of diverse species including humans and yeast (Table 1, and see Refs. [3,9,35]). The TBW VDAC protein has a single-channel conductance of 4.1 nS in 1 M KCl, identical to that observed for *D. melanogaster* [18]. TBW channels closed in response to increasing positive and negative transmembrane potentials. It should be pointed out that although VDACs present a formidable barrier to the movement of organic anions in the closed state, they remain permeable to small ions (T. Rostovtseva and M. Colombini, unpublished data). The reversal potential of 11.8 mV indicates that in the open state TBW channels are anion selective as for VDACs from diverse species. The possibility that gap junction channels contribute to the biophysical recordings is unlikely since connexons must insert and pair in adjacent membranes for functionality and gap junction conductance differs from that for VDACs in 1 M KCl (reviewed in [37]). The failure of NaOH-extracted, filtered, OG-solubilized fractions to form VDAC channels in vitro either with or without the addition of detergents may be due to structural changes in the structure of the protein which preclude appropriate membrane insertion or charge carrying function.

The TBW VDAC protein was exceptionally immunogenic in a rabbit, yielding an antiserum (R19) which reacted strongly with the 31 kDa protein on Western blots at antibody dilutions as great as 1:500 000. In addition, R19 and the affinity-purified R19AP stain 31 kDa proteins on immunoblots of tissue homogenates from a mammal, an insect cell line, four orders of insects, three non-insect arthropods, an annelid and several species of plants (J. Ryerse, unpublished data), indicate the wide spectrum of cross-reactivity of the antibody and the conservation of VDACs across the plant and animal kingdoms. However, homogenates of *S. cerevisiae* and *D. discoideum* stained lightly or not at all. Recently, an antibody was raised against *D. melanogaster* VDAC protein for library screens [19] but no details of cross-reactivity with other species were reported. Antibodies against VDACs from four different species were tested for cross-reactivity on blots of *D. melanogaster* homogenates, with no (*N. crassa*), weak (bovine heart), strong (yeast) or moderate (human VDAC peptide) immunoreactivity being observed [18,38].

Immunocytochemistry provided another line of evidence that the TBW 31 kDa protein is a VDAC protein. Both R19 and R19AP specifically stain mitochondria in TBW flight muscle by immunofluorescence and immunogold cytochemistry. At the LM level, distinct staining of the mitochondrial periphery was more pronounced with R19AP (Fig. 7D) than with R19 (Fig. 7B) due to reduced background staining. At the EM level, R19AP stained peripheral mitochondrial membranes in LR White-embedded tissue sections (Fig. 7F), however, fragmentation and partial dissolution of membranes due to extraction in the absence of osmium fixation made it impossible to determine if the staining was specific for the inner or outer membrane. In contrast, in ultrathin cryo-sections the mitochondrial periphery stained intensely with R19AP and colloidal gold-labelled secondary antibody (Fig. 7G) and in areas where the membranes were exactly cross-sectioned, the localization was specific for the outer membrane (arrows in Fig. 7G).

Taken together, the data on molecular mass, N-terminal sequence, biophysical properties and tissue immunocytochemistry show that the TBW 31 kDa protein is a VDAC family member. The R19AP antibody was used as a probe in an expression screen to isolate a *D. melanogaster* VDAC cDNA which is molecularly characterized in the companion paper [20].

Acknowledgements

We thank Monsanto Company for supplying the *Heliothis virescens* and carrying out N-terminal amino acid sequencing.

References

[1] M. Colombini, Nature 279 (1979) 643–645.
[2] M. Colombini, in: W.G. Guggino (Ed.), Current Topics in Membranes, vol. 42, Academic Press, San Diego, 1994, chapter 4, pp. 73–101.
[3] M. Colombini, E. Blachly-Dyson and M. Forte, in: T. Narahashi (Ed.), Ion Channels, vol. 4, Plenum Press, New York, 1996, pp. 169–202
[4] D. Levitt, Curr. Opin. Cell Biol. 2 (1990) 689–694.
[5] C. Mannella, Trends Biol. Sci. 17 (1992) 315–320.
[6] S. Alziari, G. Stepen, R. Durand, Biochem. Biophys. Res. Commun. 91 (1981) 1–8.
[7] V. De Pinto, O. Ludwig, J. Kraus, R. Benz, F. Palmieri, Biochim. Biophys. Acta 894 (1987) 109–119.
[8] E. Blachly-Dyson, S. Peng, M. Colombini, M. Forte, Science 247 (1990) 1233–1236.
[9] M. Colombini, J. Membr. Biol. 111 (1989) 103–111.
[10] E. Blachly-Dyson, E. Zambronicz, W. Yu, V. Adams, E. McCabe, J. Adelman, M. Colombini, M. Forte, J. Biol. Chem. 268 (1993) 1835–1841.
[11] D. Brdiczka, Experientia 46 (1990) 161–167.
[12] M. Liu, M. Colombini, J. Bioenerg. Biomembr. 24 (1992) 41–46.
[13] M. Liu, M. Colombini, Biochim. Biophys. Acta 1098 (1992) 255–260.
[14] M. Zizi, M. Forte, E. Blachly-Dyson, M. Colombini, J. Biol. Chem. 269 (1994) 1614–1616.
[15] A. Lee, M. Zizi, M. Colombini, J. Biol. Chem. 269 (1994) 30974–30980.
[16] H. Florke et al., Biol. Chem. Hoppe-Seyler's 375 (1994) 513–520.
[17] G. Rubin, Science 240 (1988) 1453–1459.
[18] V. De Pinto, R. Benz, C. Caggese, F. Palmieri, Biochim. Biophys. Acta 987 (1989) 1–7.
[19] A. Messina, M. Neri, F. Perosa, C. Caggese, M. Marino, R. Caizzi, V. De Pinto, FEBS Lett. 384 (1996) 9–13.
[20] J. Ryerse, E. Blachly-Dyson, M. Forte, B. Nagel, Biochim. Biophys. Acta 1327 (1997) 204–212.
[21] J. Ryerse, Cell Tissue Res. 274 (1993) 393–403.
[22] J. Ryerse, Tissue Cell 27 (1995) 349–353.
[23] J. Ryerse, Cell Tissue Res. 256 (1989) 7–16.
[24] P. Matsudaira, J. Biol. Chem. 262 (1987) 10035–10038.
[25] M. Montal, P. Mueller, Proc. Natl. Acad. Sci. USA 69 (1972) 3561–3566.
[26] M. Colombini, in: L. Packer, R. Douce (Eds.), Plant Cell membranes; Methods in Enzymology, vol. 148, Academic Press, Orlando, 1987, pp. 465–475.
[27] K. Tokuyasu, J. Cell Biol. 57 (1973) 551–565.
[28] K. Tokuyasu, Histochem J. 12 (1980) 381–403.
[29] E. Hertzberg, J. Biol. Chem. 259 (1984) 9936–9943.
[30] C. Mannella, in: M. Forte, M. Colombini (Eds.), Molecular Biology of Mitochondrial Transport Systems, NATO ASI Series, vol. H83, Springer Verlag, Berlin, 1994, pp. 249–263.
[31] P. Rosevear, T. VanAken, J. Baxter, S. Ferguson-Miller, Biochemistry 19 (1980) 4108–4115.
[32] H. Ha, P. Hajek, D. Bedwell, P. Burrows, J. Biol. Chem. 268 (1993) 12143–12149.
[33] M. Colombini, J. Membr. Biol. 53 (1980) 79–84.
[34] C.A. Mannella, M. Colombini, J. Frank, Proc. Natl. Acad. Sci. USA 80 (1983) 2243–2247.
[35] A. Blumenthal, K. Kahn, O. Beja, E. Galun, M. Colombini, A. Breiman, Plant Physiol. 101 (1993) 579–587.
[36] J. Ryerse, Tissue Cell 23 (1991) 709–718.
[37] J. Ryerse, in: F. Harrison, M. Locke (Eds.), Microscopic Anatomy of Invertebrates, vol. 11, Wiley-Liss, New York, 1996, in press.
[38] V. De Pinto, V. Zara, R. Benz, G.V. Gnoni, F. Palmieri, Biochim. Biophys. Acta 1061 (1991) 279–286.
[39] L. Jurgens, P. Ilsemann, H. Kratzin, D. Hesse, K. Eckart, F. Thinnes, N. Hilschmann, Biol. Chem. Hoppe- Seyler's 372 (1991) 455–463.
[40] M. Bureau, M. Khrestchatisky, M. Heeren, E. Zambrowicz, H. Kim, T. Grisar, M. Colombini, A. Tobin, R. Olsen, J. Biol. Chem. 267 (1992) 8679–8684.
[41] L. Heins, H. Mentzel, A. Schmid, R. Benz, U. Schmitz, J. Biol. Chem. 269 (1994) 26402–26410.
[42] K. Fischer, A. Weber, S. Brink, B. Arbinger, D. Schunemann, S. Bochert, H. Held, B. Popp, R. Benz, T. Link, C. Eckerskorn, U. Flugge, J. Biol. Chem. 269 (1994) 25754–25760.
[43] H. Troll, D. Malchow, A. Muller-Taubenberger, B. Humbell, F. Lottspeich, M. Ecke, G. Gerisch, A. Schmid, R. Benz, J. Biol. Chem. 267 (1992) 21072–21079.
[44] R. Kleene, N. Pfanner, R. Pfaller, T. Link, W. Sebald, W. Neupert, M. Tropschug, EMBO J. 6 (1987) 2627–2633.
[45] M. Forte, H. Guy, C. Mannella, J. Bioenerg. Biomembr. 19 (1987) 341–350.